Supplementary Information

Flavonoids improve the stability and function of P23H rhodopsin, and slow down the progression of retinitis pigmentosa in mice

Joseph T. Ortega[1], Tanu Parmar[1], Miguel Carmena-Bargueño[2], Horacio Pérez-Sánchez[2#] and Beata Jastrzebska[1#]

[1]Department of Pharmacology, Cleveland Center for Membrane and Structural Biology, School of Medicine, Case Western Reserve University, 10900 Euclid Ave., Cleveland, OH 44106, USA

[2]Structural Bioinformatics and High Performance Computing Research Group (BIO-HPC), UCAM Universidad Católica de Murcia, Guadalupe 30107, Spain

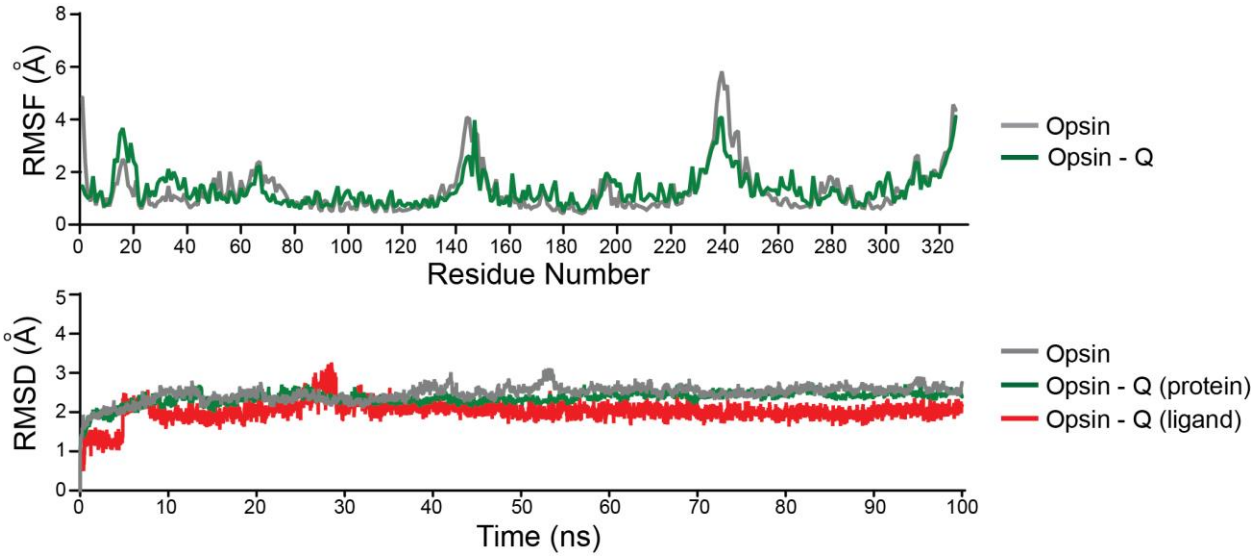

Figure S1. The binding stability of quercetin within the orthosteric binding pocket of WT Rho. WT rod opsin (PDB ID: 3CAP) alone or in the complex with quercetin was subjected to the molecular dynamic (MD) simulations. **A**, The root-mean-square fluctuations (RMSF) were plotted with respect to the residue number of rod opsin. **B,** The root-mean-square deviations (RMSD) were plotted for WT opsin and WT opsin with bound quercetin (grey and green plots, respectively) with respect to the initial pose. Also, the RMSD for the ligand bound to WT opsin is shown (red plot).

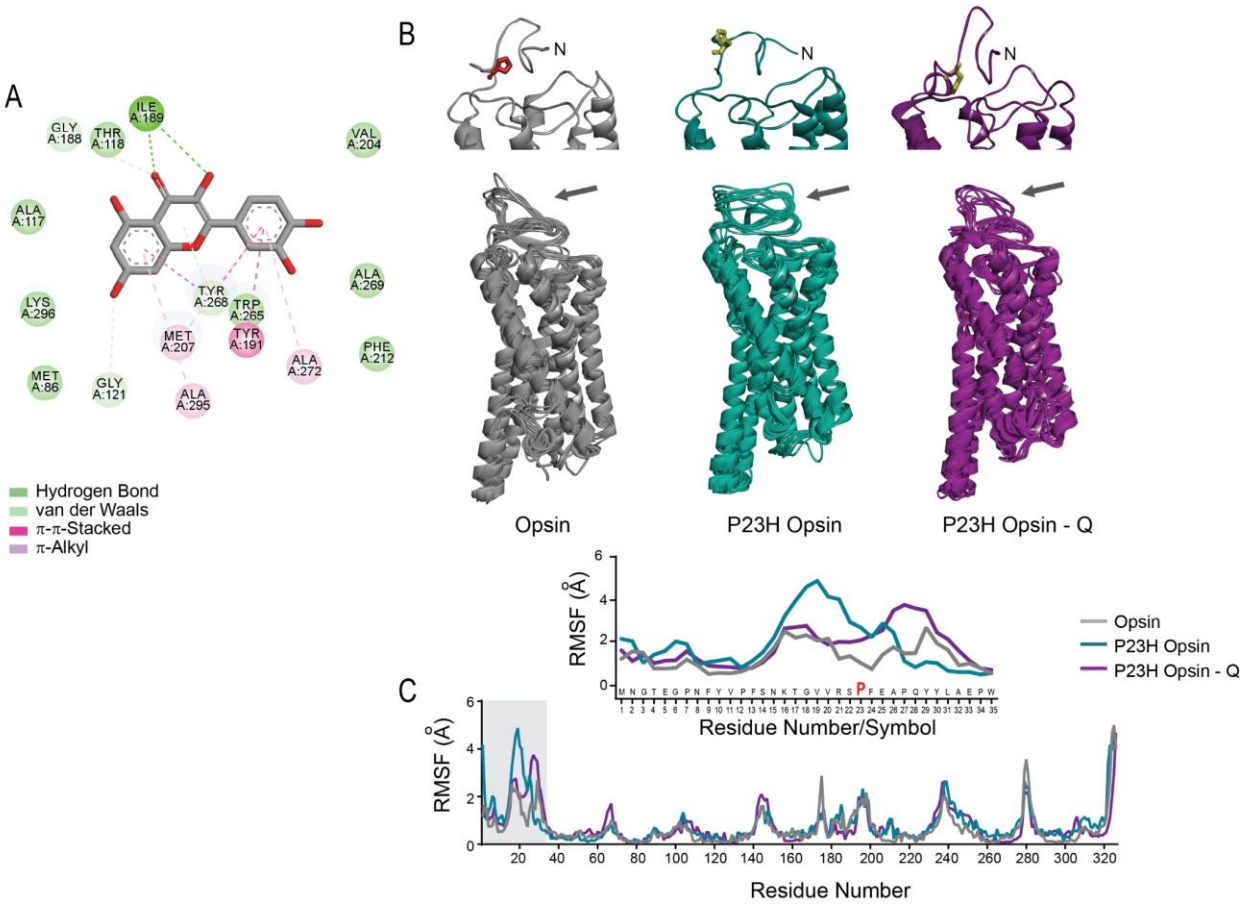

Figure S2. The effect of flavonoids on the conformational stability of P23H Rho. A, The molecular docking of quercetin to P23H rod opsin model was conducted with VINA/VegaZZ using the orthosteric binding site parameters of rod opsin as described in (Ortega et al., 2019). The main interactions of quercetin with the residues in the orthosteric site of P23H rod opsin are shown. **B,** The ligand-free P23H rod opsin structure and the model of P23H rod opsin with quercetin bound were optimized and subjected to the molecular dynamic (MD) simulations carried out using CASB-Flex software. A monomer of WT rod opsin (PDB ID: 3CAP) was used as a control. The results of these MD simulations are shown. The extracellular N-terminal loop with the resident Pro23 residue is indicated with an arrow. The location of Pro23 or His23 in the final pose obtained after MD simulations is shown for each structure in the upper part of this panel. In the lower panel, ten superimposed final MD poses obtained for WT rod opsin, P23H rod opsin mutant and P23H rod opsin mutant with bound quercetin are shown. The structural flexibility of the N-terminal loop (indicated with arrow) increases upon the substitution of Pro23 to His residue. The binding of quercetin to P23H rod opsin increases its structural stability and facilitates the structural changes resembling WT-like conformation. **C,** The root-mean-square fluctuation (RMSF) plotted

with respect to the residue number of rod opsin. The N-terminal loop residues are highlighted with a gray bar. *Inset*, a close-up view of the N-terminal loop residues.

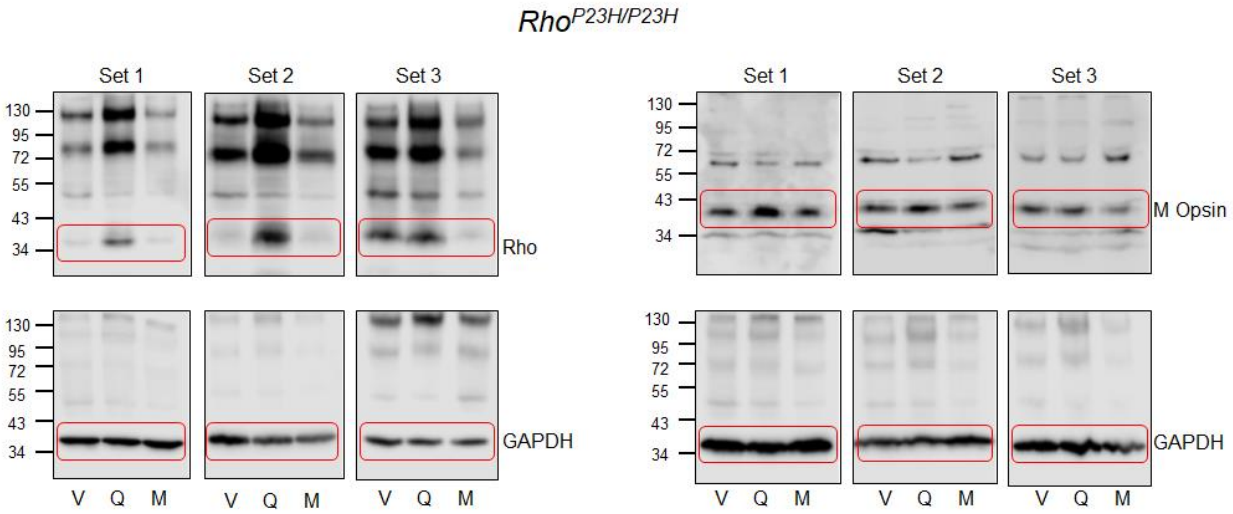

Figure S3. Immunoblot membranes. Whole eye extract from vehicle (V), quercetin (Q), or myricetin (M)-treated homozygous *Rho*$^{P23H/P23H}$ mice used for quantification of the protein expression of Rho and M cone opsin shown in Figure 4D. Quantified protein bands are indicated with red rectangular.

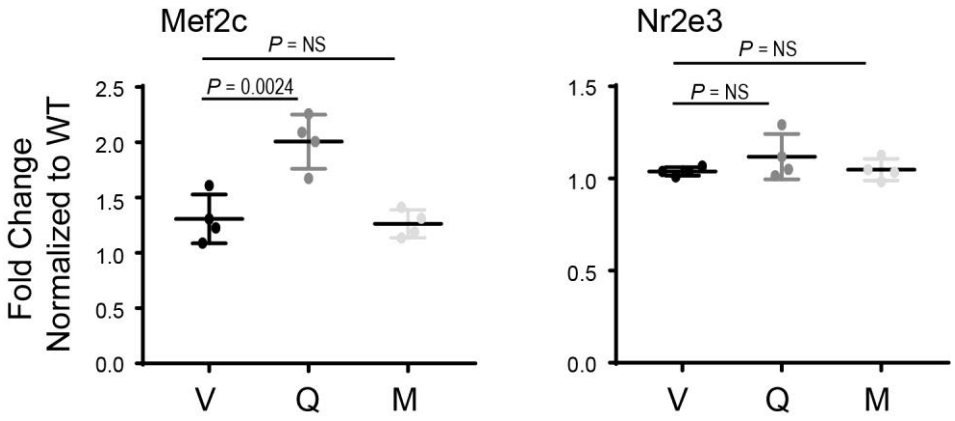

Figure S4. The effect of flavonoids on the expression of transcription factors *Mef2c* and *Ner2*. The expression levels of *Mef2c* and *Nr2e3* transcription factors that regulate the expression of Rho and cone opsins were examined with RT-qPCR; three runs were performed (*Mef2c*, n = 3, $F_{2,9}$ = 16.74, P = 0.0009; *Nr2e3*, n = 3, $F_{2,9}$ = 1.19, P = 0.3468).Total RNA was isolated from the eyes of $Rho^{P23H/P23H}$ mice treated with either vehicle or flavonoids collected at P21. Relative fold change of these genes' expression was normalized to the expression of *Gapdh*. Error bars indicate standard deviation (S.D). The expression of *Mef2c* was significantly different only upon treatment with quercetin but not myricetin. No change was found for the expression of *Nr2e3*. The *P*-value for statistically different changes between flavonoid-treated and vehicle-treated mice is indicated in the figure. The non-statistically different changes are indicated as NS. Statistical analysis was performed for each gene separately, using one-way ANOVA analysis and Bonferroni post hoc tests.

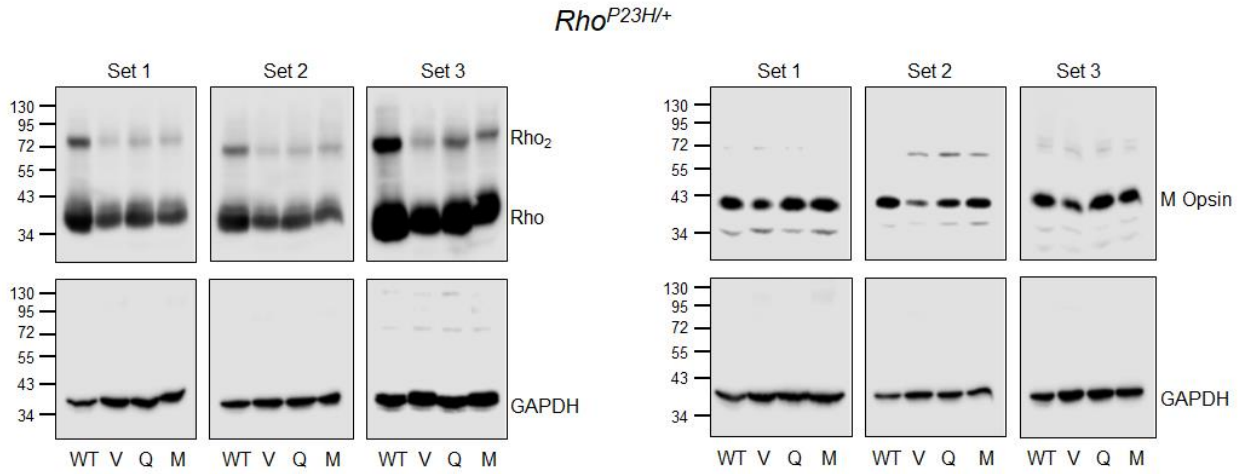

Figure S5. Immunoblot membranes. Whole eye extract from WT mice and vehicle (V), quercetin (Q), or myricetin (M)-treated heterozygous *Rho*$^{P23H/+}$ mice used for quantification of the protein expression of Rho and M cone opsin shown in Figure 7D.

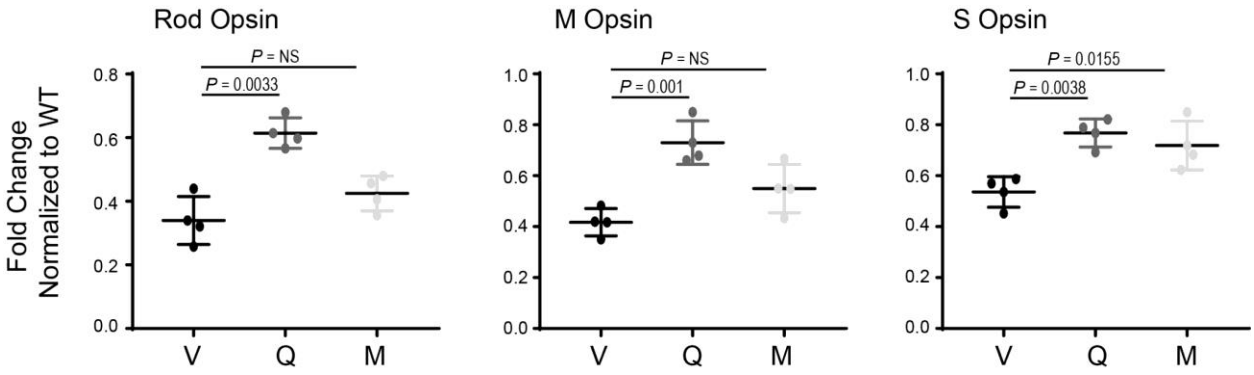

Figure S6. The effect of flavonoids on the Rho and cone opsin gene expression in *Rho*$^{P23H/+}$ mice. The expression levels of genes encoding rod opsin, M cone opsin, and S cone opsin were examined with RT-qPCR; three runs were performed (rod opsin, $n = 3$, $F_{2,9} = 21.67$, $P = 0.0004$; M opsin, $n = 3$, $F_{2,9} = 15.30$, $P = 0.0013$; S opsin, $n = 3$, $F_{2,9} = 11.25$, $P = 0.0036$). At P33 eyes were collected and total RNA was isolated from the eyes of *Rho*$^{P23H/+}$ mice treated with either vehicle or flavonoids. Relative fold change of these genes' expression was normalized to the expression of *Gapdh*. Error bars indicate standard deviation (S.D.). The change in the expression of the Rho and M cone opsin genes was significantly different upon treatment with quercetin, while the expression of the S cone opsin gene was significantly upregulated upon treatment with both flavonoids in comparison to vehicle-treated mice. The *P*-values for statistically different changes are indicated in the figure. The non-statistically different changes are indicated as NS. Statistical analysis was performed for each gene separately, using one-way ANOVA analysis and Bonferroni post hoc tests.

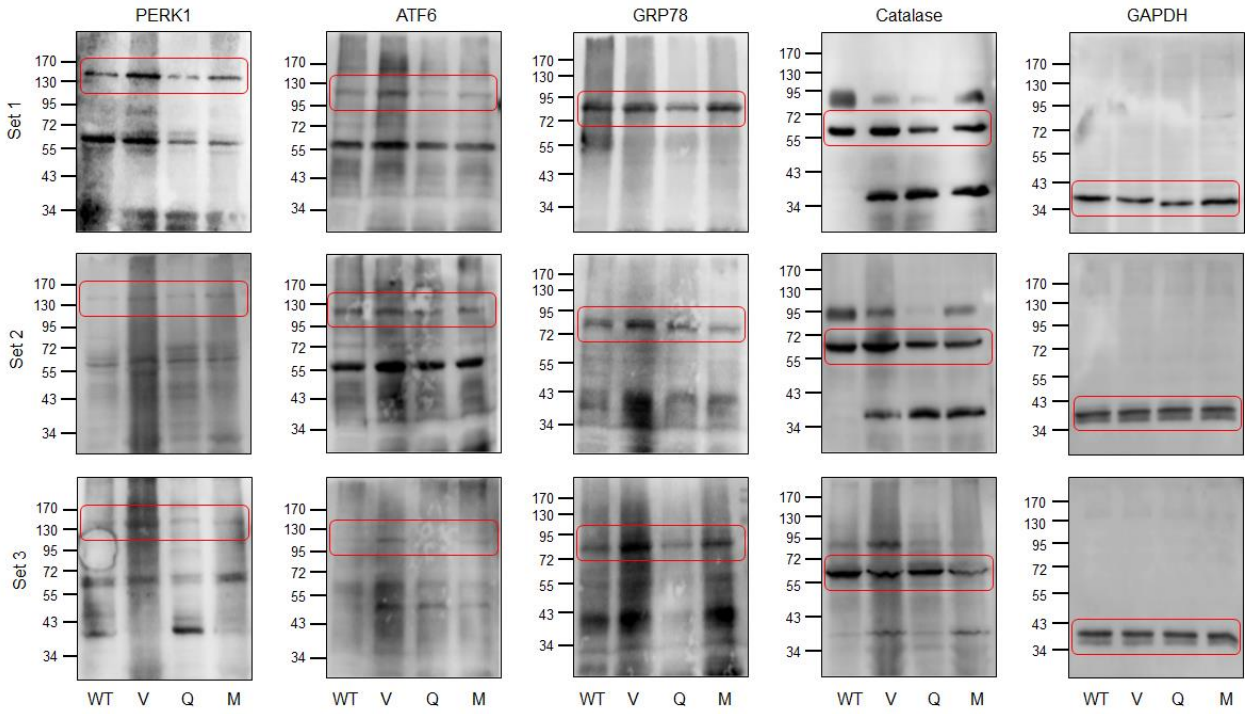

Figure S7. Immunoblot membranes. Whole eye extract from WT mice and vehicle (V), quercetin (Q), or myricetin (M)-treated heterozygous P23H Rho mice used for quantification of the UPR stress markers protein expression shown in Figure 8D. Quantified protein bands are indicated with red rectangular.

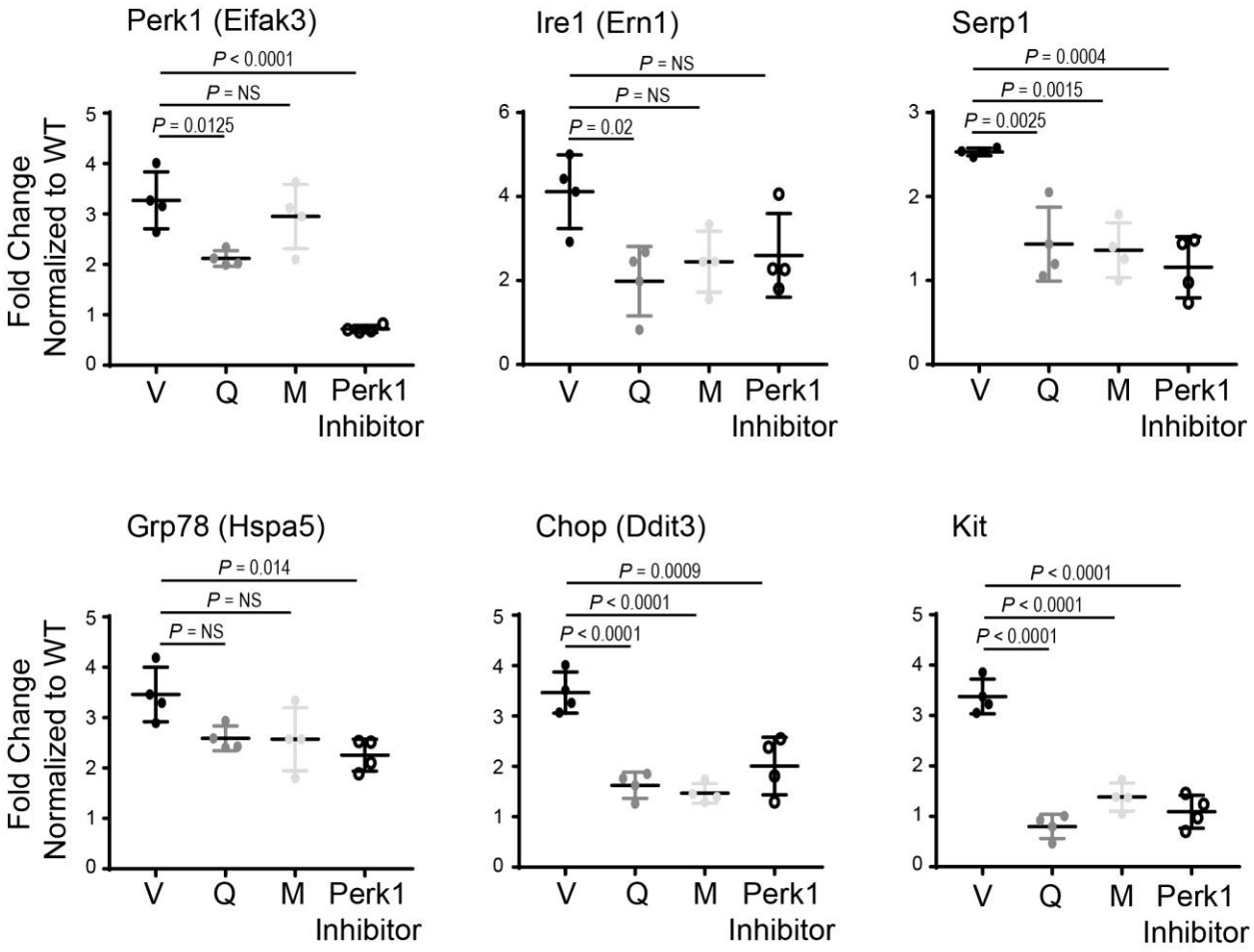

Figure S8. The effect of flavonoids on stress response in P23H Rho-expressing cells. The expression levels of selected UPR stress-related markers were examined in the NIH-3T3 cells stably expressing P23H Rho treated with flavonoids by RT-qPCR; three runs were performed (*Perk1*, $n = 3$, $F_{3,12} = 27.69$, $P < 0.0001$; *Ire1*, $n = 3$, $F_{3,12} = 4.59$, $P < 0.0232$; *Serp1*, $n = 3$, $F_{3,12} = 14.00$, $P = 0.0003$, *Grp78*, $n = 3$, $F_{3,12} = 5.04$, $P = 0.0137$; *Chop*, $n = 3$, $F_{3,12} = 22.24$, $P < 0.0001$; *Kit*, $n = 3$, $F_{3,12} = 60.79$, $P < 0.0001$). Either total RNA was isolated from cells treated with flavonoids or the vehicle Relative fold change of these genes' expression was normalized to the expression of *Gapdh*. The change in the expression of the analyzed genes was significantly reduced upon treatment with both flavonoids. Error bars indicate standard deviation (S.D.). The *P*-values for statistically different changes are indicated in the figure. NS, not statistically different. Statistical analysis was performed for each gene separately, using one-way ANOVA analysis and Bonferroni post hoc tests. V, treated with vehicle, Q, treated with quercetin, M, treated with myricetin.

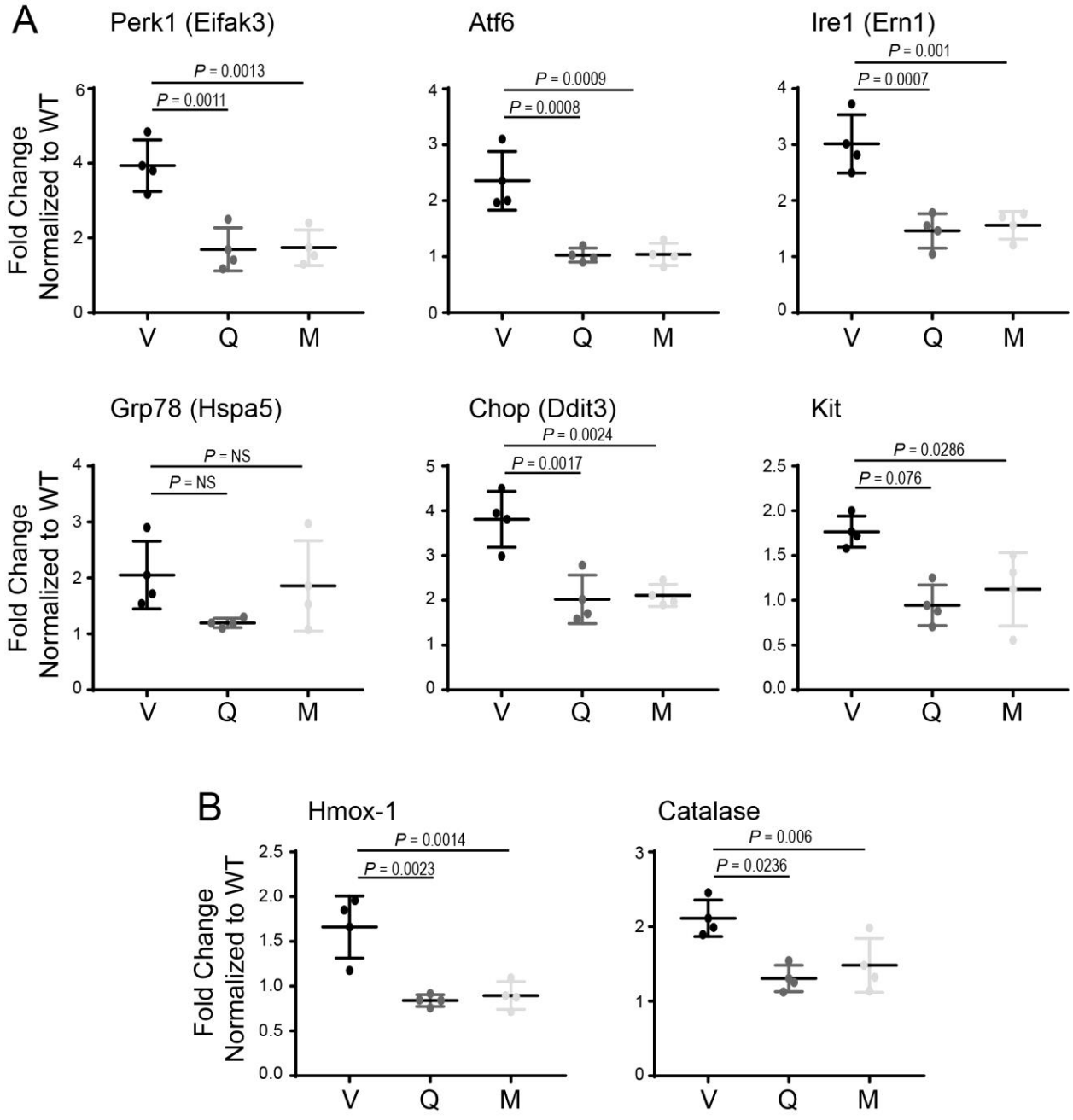

Figure S9. The effect of flavonoids on stress response in *Rho*$^{P23H/+}$ mice related to a P23H mutation in Rho. The expression levels of selected UPR stress-related (**A**) and oxidative stress-related genes (**B**) were examined by RT-qPCR; three runs were performed (*Perk1*, $n = 3$, $F_{2,9} = 19.07$, $P = 0.0006$; *Atf6*, $n = 3$, $F_{2,9} = 21.12$, $P = 0.0004$; *Ire1*, $n = 3$, $F_{2,9} = 21.24$, $P < 0.004$; *Grp78*, $n = 3$, $F_{2,9} = 2.37$, $P = 0.0004$; *Chop*, $n = 3$, $F_{2,9} = 16.33$, $P = 0.001$; *Kit*, $n = 3$, $F_{2,9} = 8.59$, $P = 0.0072$; *Hmox-1*, $n = 3$, $F_{2,9} = 17.03$, $P = 0.0066$; *Catalase*, $n = 3$, $F_{2,9} = 9.68$, $P = 0.0057$). At P33 eyes were collected and total RNA was isolated from the eyes of heterozygous *Rho*$^{P23H/+}$ mice

treated with either flavonoids or vehicle. Relative fold change of these genes' expression was normalized to the expression of *Gapdh*. Error bars indicate standard deviation (S.D.). The change in the expression of the analyzed genes was significantly reduced upon treatment with both flavonoids. The *P*-values for statistically different changes are indicated in the figure. NS, not statistically different. Statistical analysis was performed for each gene separately, using one-way ANOVA analysis and Bonferroni post hoc tests.